



DOE/NV/25946--256

# Calibrating the DARHT Electron Spectrometer with Negative Ions

November 2005

R. Trainham  
Special Technologies Laboratory

A. P. Tipton  
Los Alamos Operations

R. R. Bartsch  
Los Alamos National Laboratory

Special Technologies Laboratory  
5520 Ekwil Street, Suite B  
Santa Barbara, CA 93110

Operated by National Security Technologies, LLC, for the U.S. Department of Energy

## **DISCLAIMER**

This report was prepared as an account of work sponsored by an agency of the United States Government. Neither the United States Government nor any agency thereof, nor any of their employees, makes any warranty, expressed or implied, or assumes any legal liability or responsibility for the accuracy, completeness, or usefulness of any information, apparatus, product, or process disclosed, or represents that its use would not infringe privately-owned rights. Reference herein to any specific commercial product, process, or service by trade name, trademark, manufacturer, or otherwise, does not necessarily constitute or imply its endorsement, recommendation, or favoring by the United States Government or any agency thereof. The views and opinions of authors expressed herein do not necessarily state or reflect those of the United States Government or any agency thereof.

## ABSTRACT

Negative ions of hydrogen and oxygen have been used to calibrate the DARHT electron spectrometer over the momentum range of 2 to 20 MeV/c. The calibration was performed on September 1, 3, and 8, 2004, and it is good to 0.5% absolute, provided that instrument alignment is carefully controlled. The momentum in MeV/c as a function of magnetic field (B in Gauss) and position in the detector plane (X in mm) is:

$$P = \frac{B - 6.28}{108.404 - 0.1935 * X}.$$

## CONTENTS

	ABSTRACT .....	I
1.	INTRODUCTION .....	1
2.	EXPERIMENTAL .....	1
3.	DISCUSSION .....	3
4.	CONCLUSION.....	7
5.	ACKNOWLEDGMENTS .....	8
	REFERENCES .....	8

## 1. INTRODUCTION

Since the beginning of dual axis radiographic hydrodynamic test (DARHT) operations, a magnetic sector spectrometer has been used to measure the energy of the multi-MeV electron beam. Early measurements were to the 1 or 2% level of accuracy, and at this level, field mapping and numerical ion transport simulation are adequate to calibrate the spectrometer [1]. In recent years, however, beam transport on DARHT II has necessitated more precision in beam energy measurements and, to this end, a small spectrometer was manufactured in 1995 by EG&G. In 1996 this spectrometer was calibrated with positive ions to the 0.5% level of precision [2-3], but that calibration came with an important caveat concerning absolute energy measurements. The microwave ion source used in that calibration had a high plasma potential, so the ion energy was uncertain to a level of about 2% at the low end of the calibration range. Additionally, since the calibration was performed using positive ions, the electromagnet was operated at opposite polarity. No attempt was made to quantify the systematics of reverse polarity operation and its effects upon the final calibration.

In this report we discuss a calibration of the DARHT spectrometer to the same 0.5% level of precision by means of negative ions. The use of negative ions for the calibration resolves the concern over the ion formation energy, and it makes the use of the calibration rather straightforward because the calibration is done in the same magnetic hysteresis quadrant used in DARHT operations. These measurements were made on September 1, 3, and 8, 2004, in the Negative Ion Source Laboratory at Los Alamos Operations.

## 2. EXPERIMENTAL

The design of the EG&G spectrometer is a 60-degree magnetic sector with a turning radius of 30 cm. The energy dispersion and beam refocusing properties of this design are straightforward, and can be described by analytical geometric analysis [4-6], transfer matrix analysis [7], or numerical modeling [8-11]. The maximum magnetic field in the spectrometer is approximately 3500 Gauss, resulting in a magnetic rigidity, or  $\int B \cdot dl$ , of approximately  $1.10 \times 10^5$  Gauss-cm. This places the upper limit of measurable momentum at approximately 32 MeV/c. The lower momentum limit is determined primarily by the ability to transport a charged particle beam without loss through the spectrometer and onto the detector. For the calibration reported here, the lower limit is approximately 2 MeV/c.

The beam entrance to the spectrometer is delimited by a 15-cm-long input collimator made of graphite with a 1-mm aperture bored through it. At the exit of the spectrometer is a 20-cm drift tube leading to a detector housing containing a sapphire Cherenkov plate (or a BC400 plastic scintillator), which is inclined at an angle of 34 degrees with respect to the beam axis. Cherenkov light from the plate is imaged onto a streak camera to allow for time-dependent measurements of the electron momentum.

The Cherenkov plate is not sensitive to ions; so for our calibration, the plate is replaced by a slotted calibration mask. This mask is made of alloy 360-brass and has five 0.8-mm-wide slots cut into it, each separated by 8 mm. Behind the mask is a Burle 4869 25-mm-channeltron charged particle detector. The cone of the channeltron is typically biased at -1700 V, and its anode is grounded through a Keithley 6514 electrometer. The negative bias on the channeltron's cone serves the dual purpose of providing signal gain for ion detection and rejecting low-energy stray electrons

produced by the ion beam impact on the calibration mask. As the ion beam is swept across the calibration mask, a series of five peaks is recorded. The resulting peaks are correlated with the slots, and each peak is analyzed for the central energy.

The current to the spectrometer's electromagnet is furnished by an Agilent 6690A power supply. A Danphysik model 866-600 current probe is used to measure it. The magnetic field is measured by a Group 3 DTM-151 precision Hall gaussmeter using a DT-141-7S sensor head. The gaussmeter is rated to a precision of 0.01%, and has a calibration certificate tracing it to a nuclear magnetic resonance probe measurement which, in turn, has National Institute of Standards and Technology (NIST) traceability.

Prior to a measurement, the spectrometer's magnet is cycled completely through its hysteresis loop. During this process, the yoke section of the magnet fully saturates, but the pole pieces themselves do not. Nevertheless, the procedure is adequate to achieve reproducibility in the magnetic field setting. To set the magnet, it is ramped to 300 amps on the positive hysteresis branch, and then at 300 amps on the negative branch. Then the magnetic field is lowered to the set point for a particular energy regime and held constant while the ion energy is swept for a measurement. During a series of measurements, the magnet setting is always adjusted from a higher field to a lower field. In the event that a higher field is desired for a particular measurement, the magnet is taken completely through the hysteresis loop again, and then lowered from negative saturation to the set point.

The negative ion source is made from a copper cylinder with an internal volume of approximately  $300 \text{ cm}^3$ . Embedded in the source walls are ten rows of SmCo magnets in a "picket fence" cusp arrangement. The center of the source is a field-free region, and the magnetic cusps create a barrier to hold the plasma off the source walls. The cusps themselves form the source's anode. The cathode is a heated filament using 150 mm of 0.5-mm-diameter tantalum wire twisted into a helix and fed into the source through the top of the source cylinder. At the bottom of the cylinder is a vacuum feedthrough utilized for the gas feed and diagnostic port access for Langmuir probe measurements.

The ion extraction port is cut radially through the side of the source cylinder. Here the magnetic cusp pattern is widened in order to lower the magnetic barrier. This allows the diffusion of the source plasma toward the extractor. The magnetic field is not fully suppressed, however, and the remaining field serves as a filter, allowing only collisionally dominated cold plasma to reach the extraction port. It is in this region of cold plasma, within a few millimeters of the extraction port, that negative ions are formed. The  $\int B \cdot dl$  of the magnetic filter is approximately 100 Gauss-cm.

The ion acceleration voltage is furnished by a Glassman EW50R12 power supply, and it is measured by a Ross Instruments VD60 high-precision voltage divider in conjunction with an Agilent 34401A digital voltmeter. Both the HV-bridge and the voltmeter have NIST traceable calibration certificates. The combined errors are well below the 0.1% level, and are thus negligible.

The accelerator consists of a three-electrode electrostatic stack. The first electrode, i.e., the plasma electrode, is held at the same potential as the source walls (anode). The second electrode is the extraction electrode, and it is biased a few kilovolts positive with respect to the plasma electrode.

The third electrode is biased more positive, and serves as a focus electrode. The complete electrode stack is referenced to the ion source and, thus, is negative with respect to ground. Electrons which are co-extracted with the negative ions are swept out of the beam by the magnetic tail of the source's magnetic filter, and they are stopped at the extraction electrode. Stable negative ion beams of hydrogen and oxygen are available from 2 keV up to 50 keV.

### 3. DISCUSSION

Figure 1 shows an example of the linewidth of the hydrogen negative ion signal. This linewidth represents the resolution possible from this calibration procedure, and, here, we see that it is about 0.3%. This is the resolution expected from the convolution of the beam spot size with the width of the slot in the calibration mask. Although no measurement of the spread of the ion beam energy for this source has been made at this time, the expected energy spread of less than 0.05% is negligible compared to the spectrometer's resolution. The line widths that we measure are therefore consistent with an a priori assumption of a delta function energy spread, and the instrument resolution is dominated by the geometrical focus properties of the magnetic sector.

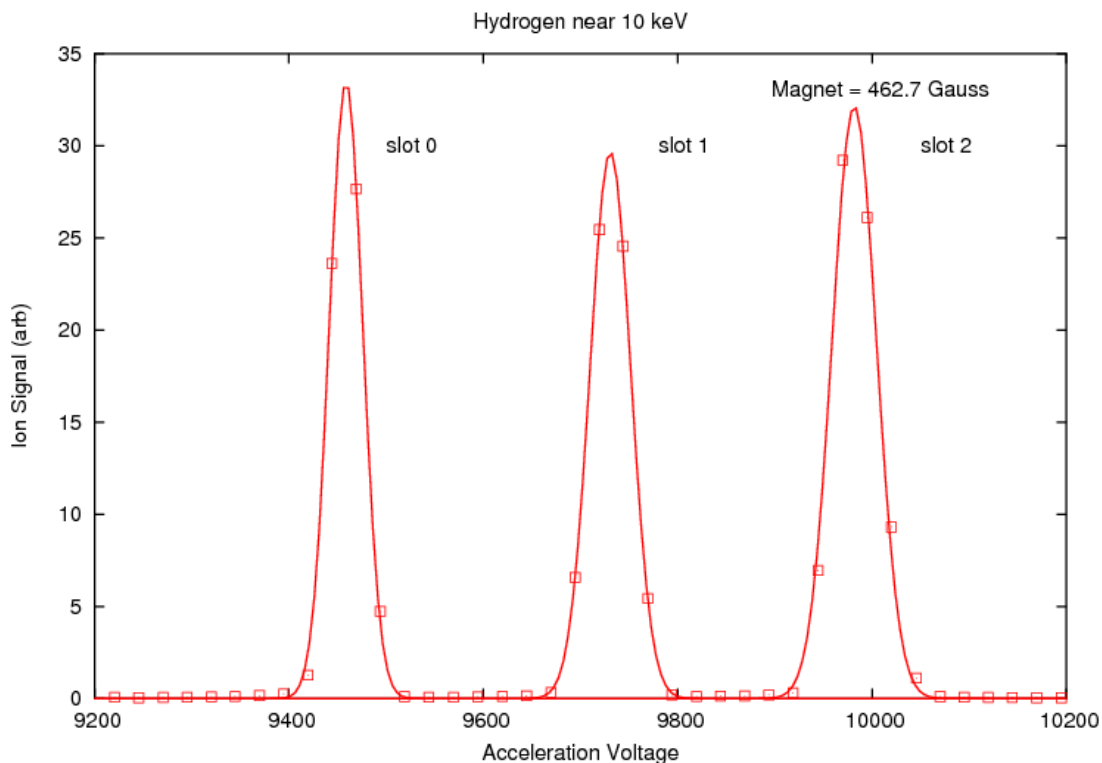


**Figure 1.** Hydrogen peaks near 10 keV, corresponding to a momentum of 4.33 MeV/c. The magnetic field is held fixed at 462.7 Gauss, and the ion beam energy is swept. The 1/e linewidth is approximately 0.3%.

Figure 2 shows an example of the oxygen negative ion signal. The linewidths are comparable to the hydrogen signals. Since our maximum acceleration voltage is 50 kV, hydrogen is suitable for only the lower half of the required calibration range of 2 to 20 MeV/c (because 50 keV hydrogen corresponds to 9.6 MeV/c). A heavier negative ion, such as oxygen, is therefore necessary to reach momenta greater than 9.6 MeV/c. The use of oxygen beams is straightforward, because  $O^-$  is a very

stable negative ion, and it forms readily in hydrogen plasmas with slight levels of air or water contamination. Only minor tuning of the extraction and focus voltages is needed to produce strong oxygen beams comparable in intensity to the hydrogen beams. In many of our oxygen data sets we find additional peaks corresponding to the  $\text{OH}^-$  molecular ion. This extra set of peaks can complicate the task of slot correlation in the analysis, but it also provides more data for the analysis.

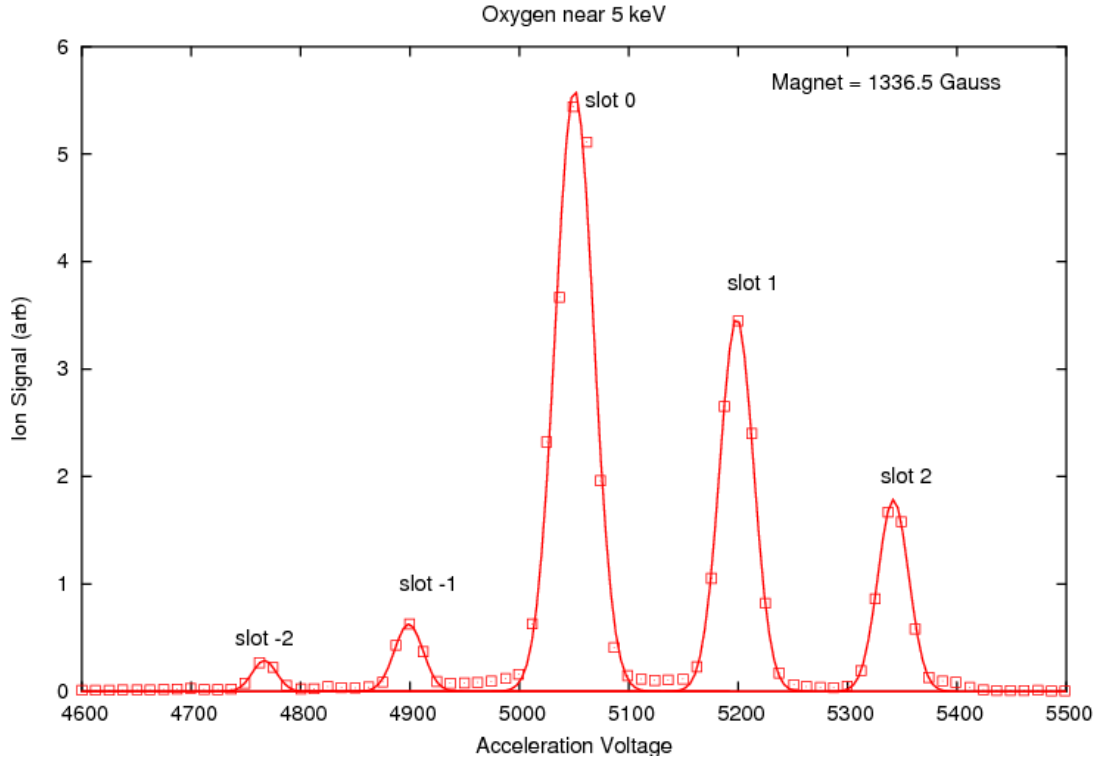


**Figure 2.** Oxygen peaks near 5 keV, corresponding to a momentum of 12.2 MeV/c. The magnetic field is held fixed at 1336.5 Gauss and the ion beam energy is swept. The  $1/e$  linewidth is approximately 0.4%.

Line centers of the ion peaks are determined by fitting the data to Gaussian profiles. These values are then converted nonrelativistically to momentum in units of MeV/c, and then the entire set of momenta is fit to the following polynomial expression:

$$P = \frac{B + A1}{A2 + A3 * X}$$

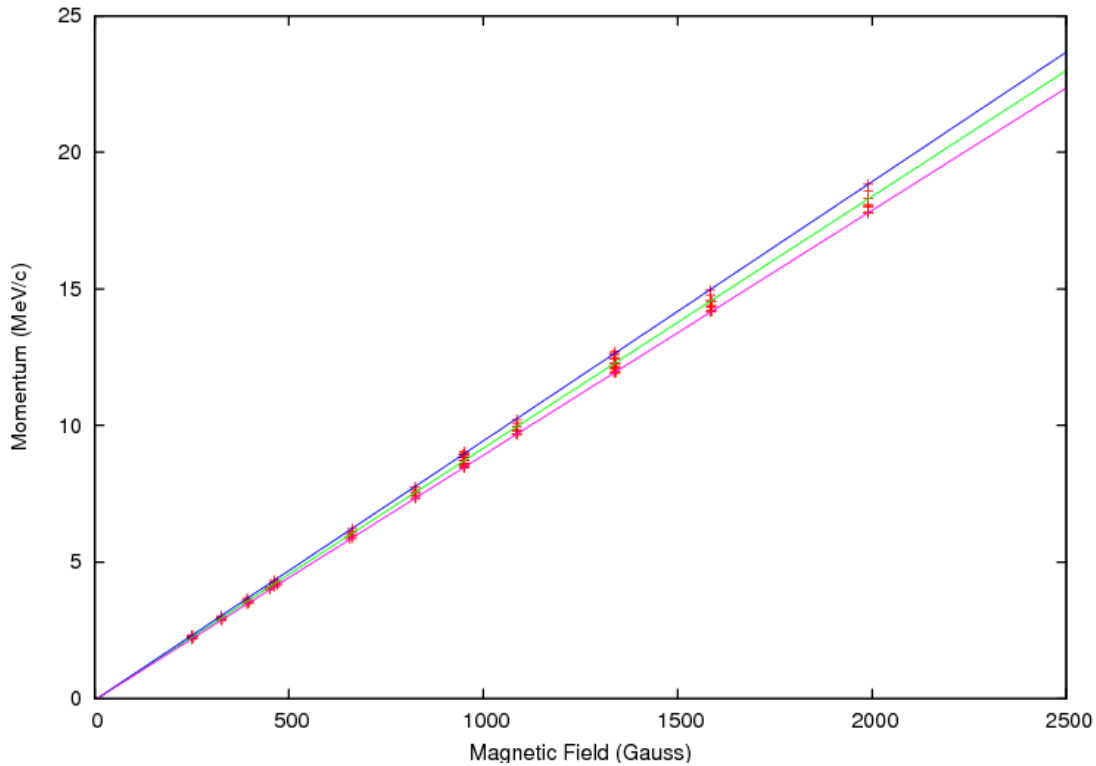
where  $A1$ ,  $A2$ , and  $A3$  are fit parameters.  $P$  is the momentum in MeV/c,  $B$  is the magnetic field in Gauss, and  $X$  is the distance in millimeters from the central beam axis in the plane of the detector. For the calibration mask used here  $X = 7.989 * N$ , where  $N$  is a particular slot number of the mask.  $N$  ranges from  $N = -2, -1, 0, 1, 2$ . The factor 7.989 is the separation in millimeters of the slots on the calibration mask. Physically,  $A1$  is simply a zero offset for the magnetic field.  $A2$  corresponds to the quantity  $1/(eR/c)$ , and  $A3$  is the linear dispersion parameter. The ratio  $A3/A2$  corresponds to the quantity  $1/(2*d*\sin(\theta))$ , where  $d$  is the effective object distance, and  $\theta$  is the magnet bending angle.



The least squares fitting procedure used is the Marquardt-Levenberg algorithm as implemented in the Gnuplot software package<sup>1</sup>. Fits which include higher orders in X or B can improve the reduced  $\chi^2$  of the fit, but yield fitting parameters that are not statistically significant for our data, and therefore are not justified. For the data set of 124 lines, the best fit parameters are:

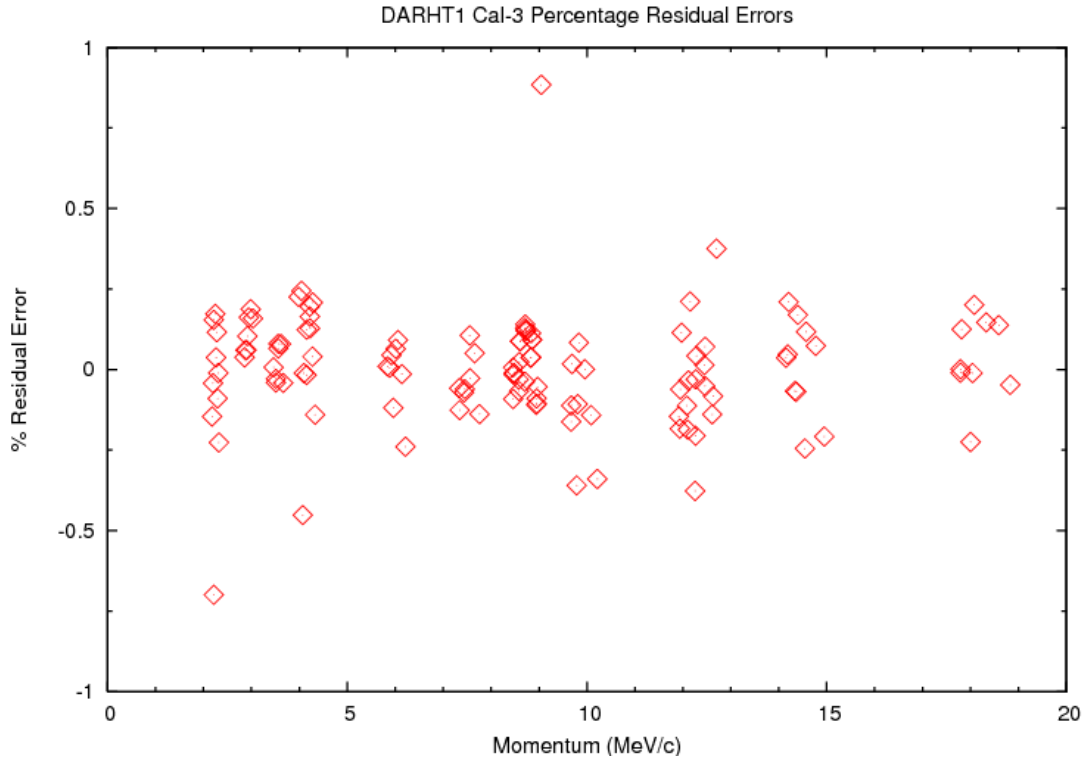
$$\begin{aligned} A1 &= -6.28 & \pm 0.33 \\ A2 &= 108.404 & \pm 0.035 \\ A3 &= -0.1935 & \pm 0.0014 \end{aligned}$$

Figure 3 shows the data plotted with the calibration fit. At each magnet setting there are five data points corresponding to the five slots in the calibration mask. The three solid curves show the calibration for the central axis and for the two calibration slots farthest from the central axis. This figure is shown to illustrate the linear nature of the calibration. Any quantitative use of the calibration should employ the polynomial representation given above. Figure 4 shows the percentage errors of the residuals of the data to the polynomial fit.



**Figure 3.** Global representation of calibration fit to the data. The upper blue line corresponds to slot 2 in the calibration mask, the center green line to slot 0, and the lower red line to slot -2

<sup>1</sup> Gnuplot is a data plotting and fitting package available from the Internet at [www.gnuplot.info](http://www.gnuplot.info). It is routinely included in all major Linux distributions.



**Figure 4.** Plot of residual percentage errors of the fit to the data. Each point is the difference of the fitted momentum from the measured momentum divided by the measured momentum and multiplied by 100.

For the fit, we have used the acceleration voltage without any corrections. Therefore, we need to consider possible effects that would make the ion energy differ from the acceleration voltage. Since the negative ions are formed within a plasma, their formation energy can be characterized by an ion temperature and a voltage potential (which is related to the plasma potential). The ion temperature is a direct contribution to the energy of the extracted ion beam. As for the potential, once the ion leaves the plasma, that potential is converted to kinetic energy. The precise region of negative ion formation for the extracted ions is uncertain, and there are two physical models for negative ion production which yield different results for the formation energies. Those models are volume production via molecular dissociation, and surface conversion of monatomic ions and neutrals [12]. Both processes presumably contribute to the negative ion formation, but it is not known which process dominates. Nevertheless, regardless of which process leads to the extracted beam, both models tend to agree that the ion temperatures are on the order of 1 eV, and that the formation potential is either very near the potential of the plasma electrode, or very near the plasma potential within the magnetic filter. In either case, for our source, it is near the anode potential. Under these assumptions, the initial energy of the negative ions is negligible compared to the acceleration voltage.

We have found that the magnetic field in the spectrometer tends to drift over time, although the magnet current remains very stable. This is probably due to a combination of real field drift in the

magnet as well as a drift in the calibration of the Hall probe measuring that field. It seems likely that the drift is temperature dependent. To gauge the importance of a temperature effect, we consider the temperature-dependent behavior of the saturation magnetization,  $M(T)$ , of pure iron. This is described by the Bloch law [13], which is:

$$M(T) = M(0)(1 - aT^{3/2})$$

where  $M(0)$  is the saturation magnetization at zero Kelvin, and  $a$  is a constant. For pure iron,  $M(0)$  is 1752 gauss, and  $a$  is approximately  $3.3 \times 10^{-6}$ . At room temperature, this yields a temperature coefficient of approximately -86 ppm per degree. For a temperature change of 50°C, which is possible but unlikely for this magnet at high currents, the shift of the calibration would be about 0.4%. So we see that the temperature of the pole pieces is not a negligible effect, although it is not likely the entire explanation of the observed shifts.

The temperature drift of the Hall probe is specified at about -30 ppm per degree, which is about one third the amplitude of the pole piece effect, and is in the same direction. This tends to exacerbate the temperature effect to the extent that a 50 degree rise in temperature of the electromagnet could result in a shift of the calibration of nearly 0.6%. One thing worth noting, however, is that the temperature drift of the Hall probe does not track with the ion energies, whereas the temperature drift of the pole pieces does. In effect, the expected error of a calibration based upon the measurement of the magnet current is about 50% greater than that of a calibration based upon the measurement of the magnetic field.

Another consideration for the uncertainty of the calibration is the mechanical misalignment of the spectrometer axis to that of the ion beam (or the DARHT beam) axis. This misalignment can be the result of the initial installation on the beam line, the shift of components during vacuum pump-down, or by thermal mechanical drift over the course of an experimental run. Geometrical analysis of the spectrometer focusing for trajectories determined by the 7-mR acceptance angle of the input collimator yields an energy “jitter” on the order of 1%. This is somewhat disappointing because it means that the 0.5% calibration is only good while the spectrometer is left untouched. Figure 5 shows an example of the energy jitter. The reproducibility is somewhat under 1%. The large shifts are due to intentional misalignment, and the small shifts are from letting the apparatus sit idle for a few hours. There are two solutions to the alignment problem: reduce the acceptance angle of the input collimator, or increase the turning radius of the magnet (i.e., build a bigger spectrometer).

## 4. CONCLUSION

Negative ions of hydrogen and oxygen have been used to calibrate the DARHT electron spectrometer over the momentum range 2 to 20 MeV/c to a precision of 0.5% absolute. The use of negative ions for the calibration removes the uncertainty of the contribution of the ion's formation energy to its final energy. It also eliminates the uncertainty of applying a calibration done in one quadrant of the spectrometer's magnetic hysteresis loop to DARHT beam operations done in another quadrant. Additionally, calibrations which use only the magnet current are not good for precisions of 1% or better. The origin of this loss of precision is probably due to a temperature drift of the magnetic susceptibility of iron pole pieces of the electromagnet. Finally, control of the mechanical alignment of the spectrometer is an important issue for calibrations to better than 1%.

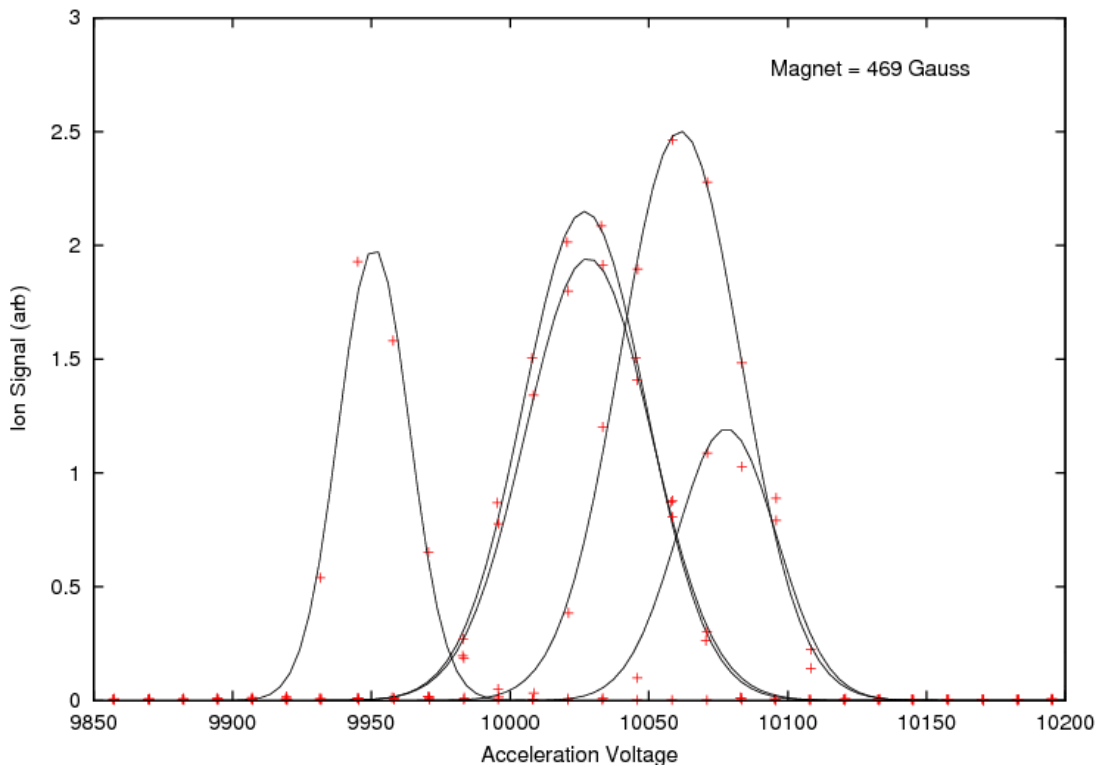


**Figure 5.** Example of calibration jitter involving mechanical misalignment and temperature drift. The large (full linewidth) shifts are from intentional misalignment of the spectrometer. The smaller (fractional linewidth) shifts are from letting the apparatus sit idle for a few hours.

## 5. ACKNOWLEDGMENTS

We would like to express our thanks to Tom Keenan and Wayne Lenhard for their mechanical design work on the ion source test stand; to Glen Anthony and Mike Celmins for their expert machining of many of the ion source parts; to Carl Carlson and Ron Sturges for helping out in the laboratory; and to Howard Bender, Carl Ekdahl, and David Oro for many fruitful discussions and their encouragement throughout this work.

## REFERENCES

1. Allison, P., "Electron-Energy Spectrometer Calibration." DARHT Technical Notes No. 17, LANL, July 16, 1991.
2. Fulton, R. D., "DARHT Spectrometer Calibration," LANL Memorandum P-22-96-U-77 (May 20, 1996).
3. Russell, S., "Analysis of THOR Spectrometer Magnet Field Map," LANL Memorandum LANSCE-9:FY01-03 (October 26, 2000).
4. Demster, A. J., "A New Method for Positive Ray Analysis", *Phys. Rev.* 11, 316 (1918).
5. Stephens, W. E., "Magnetic Refocusing of Electron Paths", *Phys. Rev.* 45, 513 (1934).

6. Barber, N. F., *Proc. Leeds Phil. Soc.* 2, 427 (1933).
7. Wollnik, H., "Ion Optics in Mass Spectrometers," *J. Mass. Spectrom.* 34, 991 (1999).
8. Humphries, Jr., S., "Magnet Design for the DARHT Spectrometer," Report AA-92-05, Acceleration Associates, 42 Tierra Monte NE, Albuquerque, NM (December 1992).
9. Humphries, Jr., S., "Focal Properties of the DARHT Spectrometer," Acceleration Associates, 42 Tierra Monte NE, Albuquerque, NM (unpublished, circa 1994).
10. Barlow, D., "Field Maps of the DARHT Spectrometer Magnet," LANL Memorandum AOT-3:94-326 (November 1, 1994).
11. Barlow, D., "Point Map Measurements of the THOR Spectrometer Magnet," LANL Memorandum LANSCE-1:TNM-00-024 (May 31, 2000).
12. Forrester, T., *Large Ion Beams*, Ch. 10, John Wiley & Sons, New York (1988).
14. Van Vleck, J. H., "A Survey of the Theory of Ferromagnetism," *Rev. Mod. Phys.* 17, 27 (1945).